Supplementary Information for:

Interrogating the potential of helical aromatic foldamers for protein recognition

Sunbum Kwon,[‡a,b] Vasily Morozov,[‡a] Lingfei Wang,[‡a] Pradeep K. Mandal,[a] Stéphane Chaignepain,[c] Céline Douat,[a] and Ivan Huc*[a]

[a] Department of Pharmacy, Ludwig-Maximilians-Universität, Butenandtstraße 5-13, D-81377 Munich, Germany

[b] Department of Chemistry, Chung-Ang University, 84 Heukseok-ro, Dongjak-gu, Seoul 06974, Republic of Korea

[c] CBMN (UMR5248), Univ. Bordeaux—CNRS—IPB, 2 rue Robert Escarpit, 33600 Pessac, France

‡ These authors contributed equally

Table of contents

1. Supplementary Figures

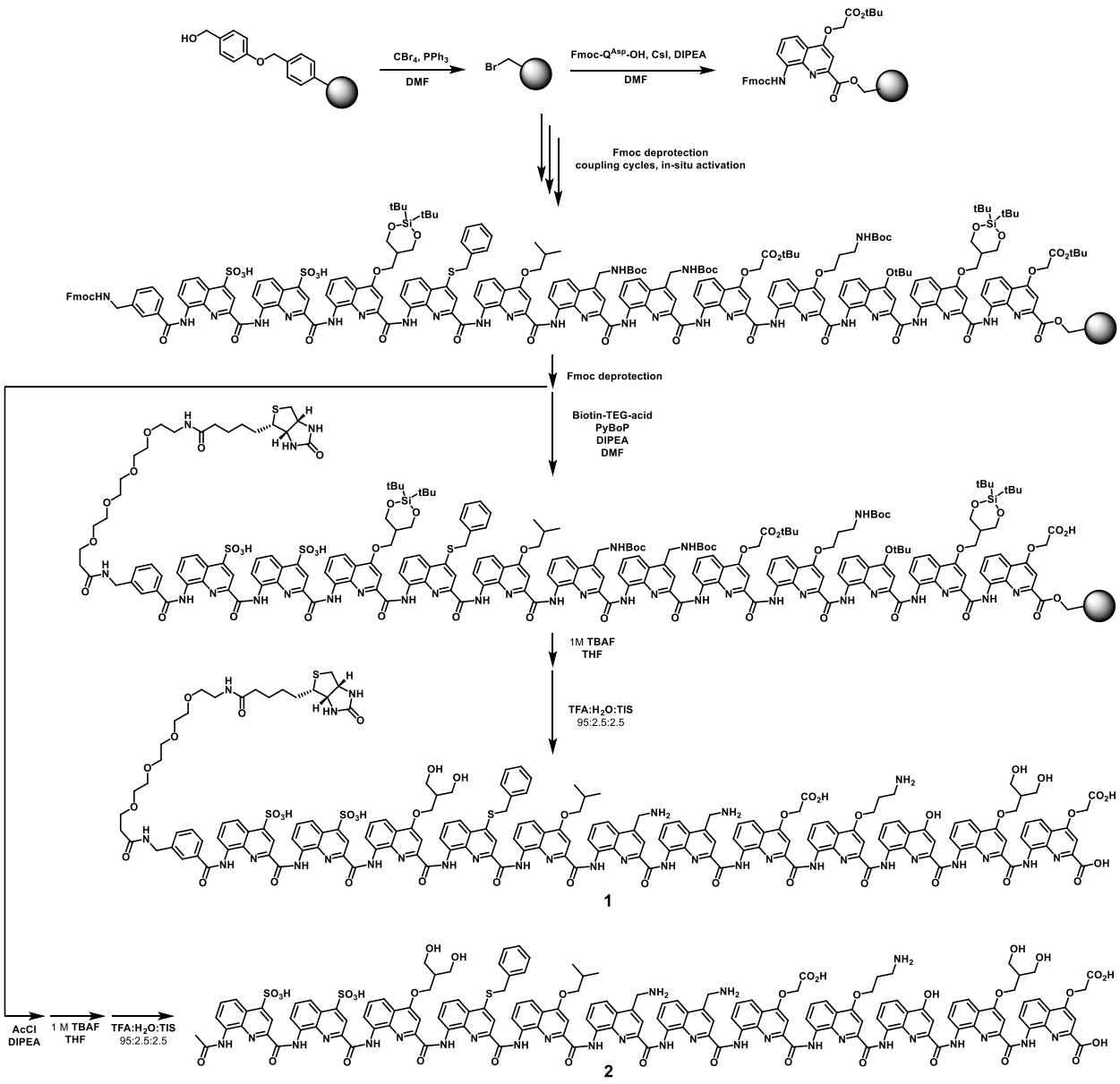

Figure S1. Solid phase synthesis of foldamers **1** and **2**.

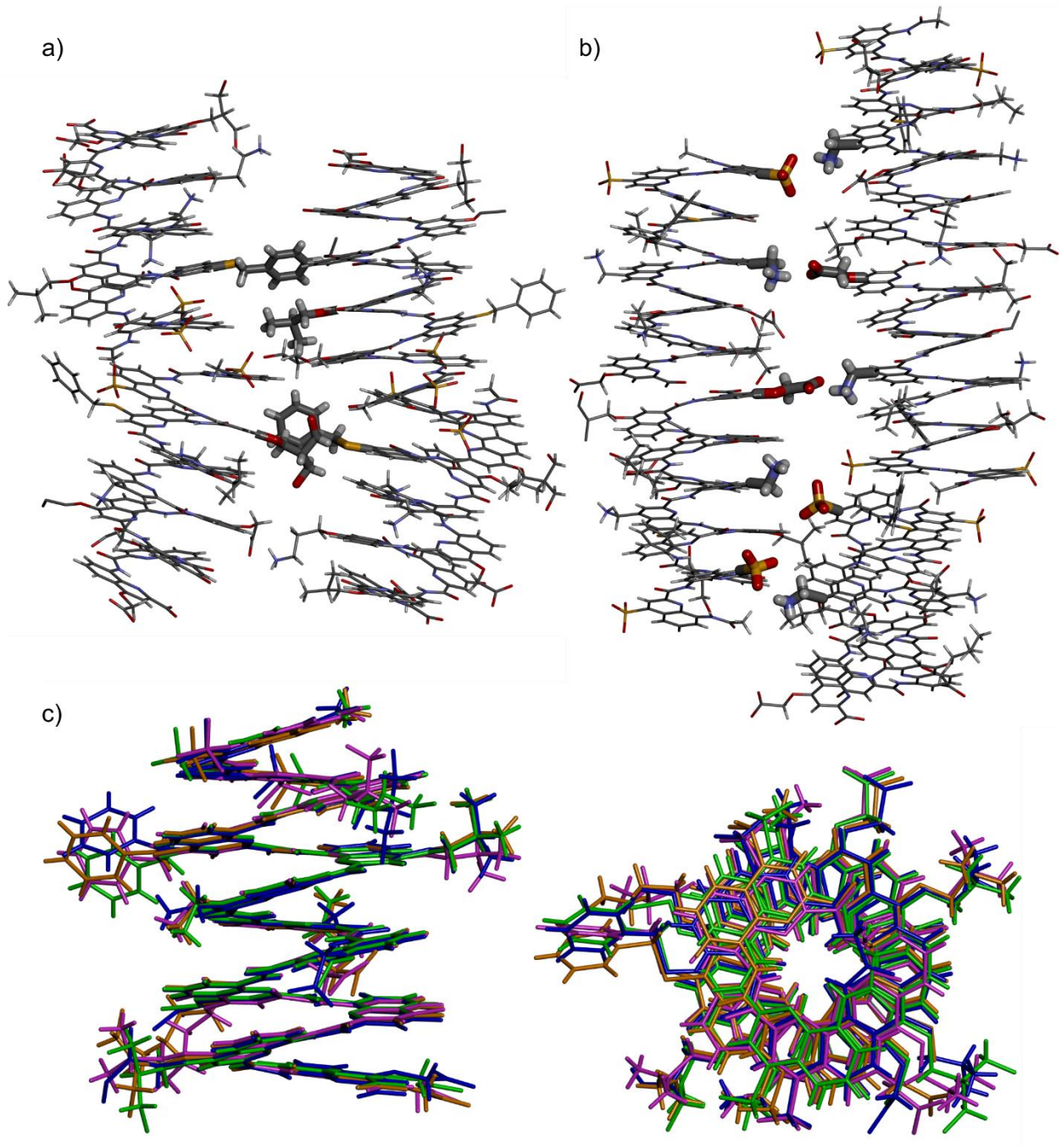

Figure S2. Crystal structure of **2**. a) Helix-helix contacts mediated by hydrophobic side chains (Q^{Phe} and Q^{Leu} or Q^{Dol}). b) Helix-helix interactions mediated by salt bridges between Q^{Dap} ammonium groups and Q^{Sul} sulfonate groups or Q^{Asp} carboxylate groups. In a) and b), the relevant side chains are shown in tube representation. c) Overlay of the main chain helix of the four crystallographically independent molecules found in the asymmetric unit.

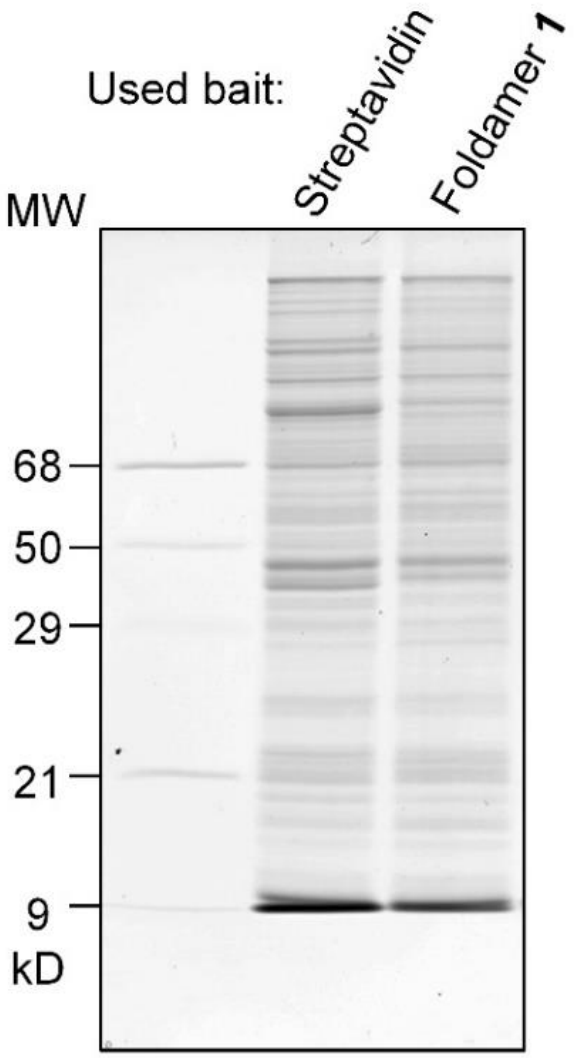

Figure S3. 10% SDS-PAGE of captured protein samples eluted from magnetic beads. The differences revealed by mass spectrometric analysis are hardly visible on the gels.

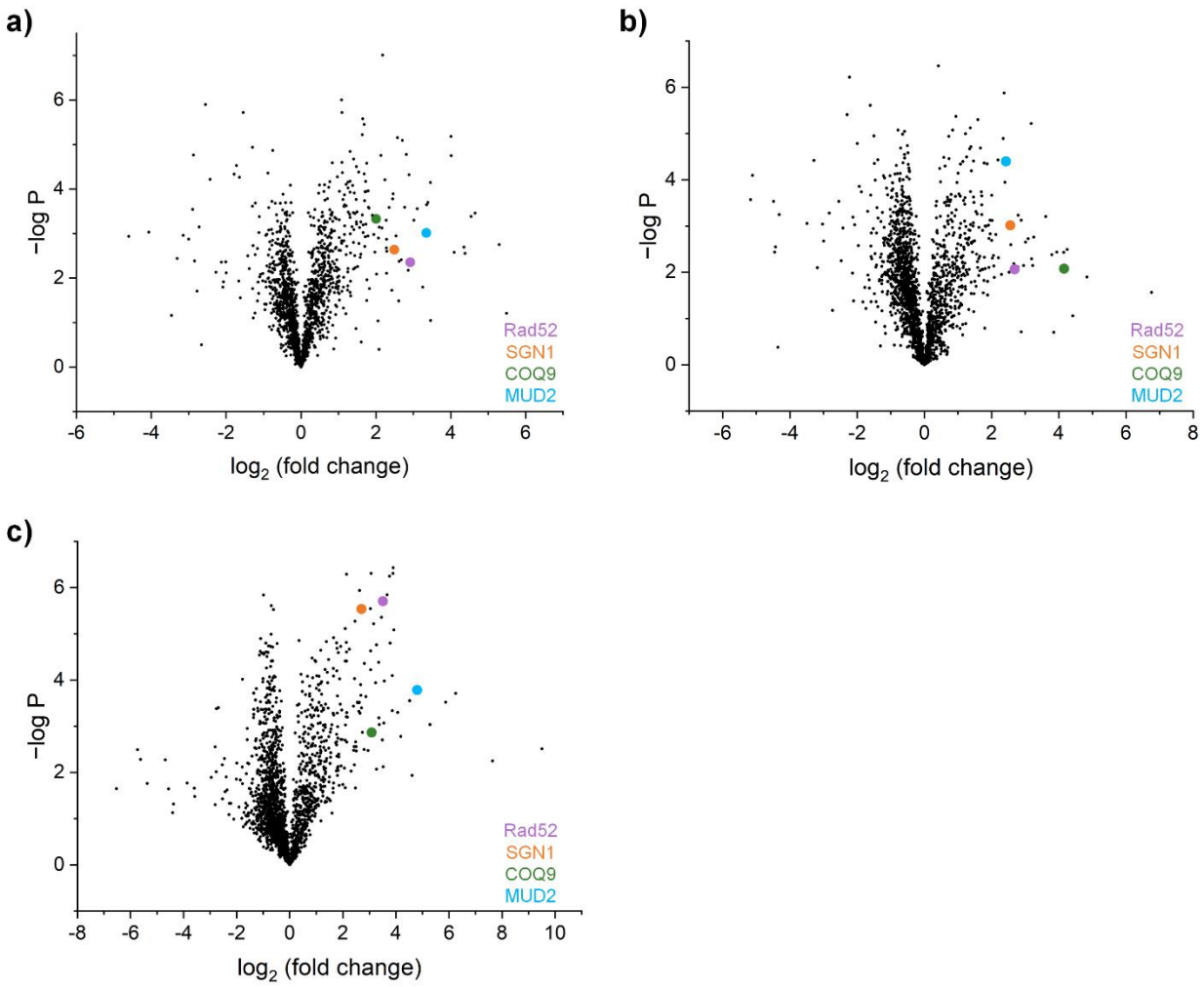

Figure S4. Volcano plots showing the significance (*y*-axis, −log P value) versus the enrichment (*x*-axis, $\log_2$ fold change) for each identified protein. Purple, orange, green and cyan dots indicate Rad52, SGN1, COQ9, and Mud2 proteins, respectively. Plots were obtained from (a) 1st, (b) 2nd and (c) 3rd pull-down experiments with foldamer **1**, respectively.

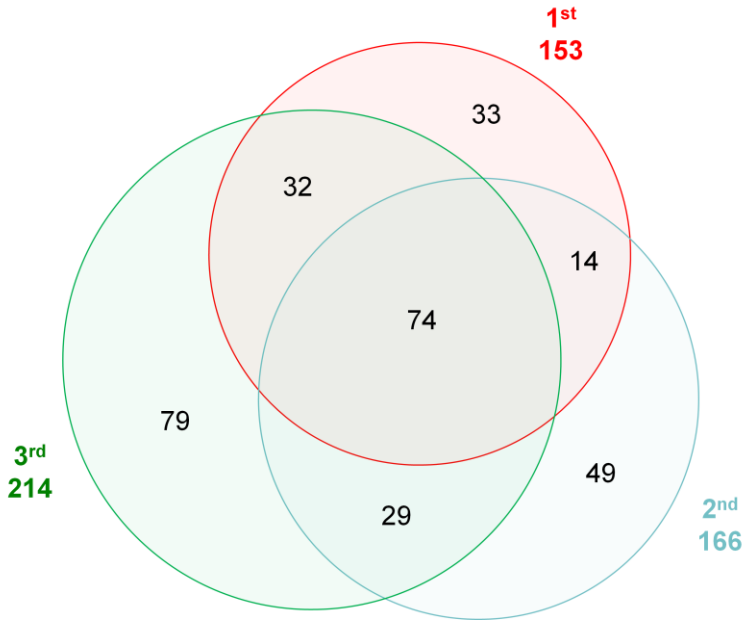

Figure S5. A Venn diagram showing the number of proteins that were enriched (fold change >2.00) when the foldamer bait was present. A total of 74 proteins exhibited enrichment across all three experiments.

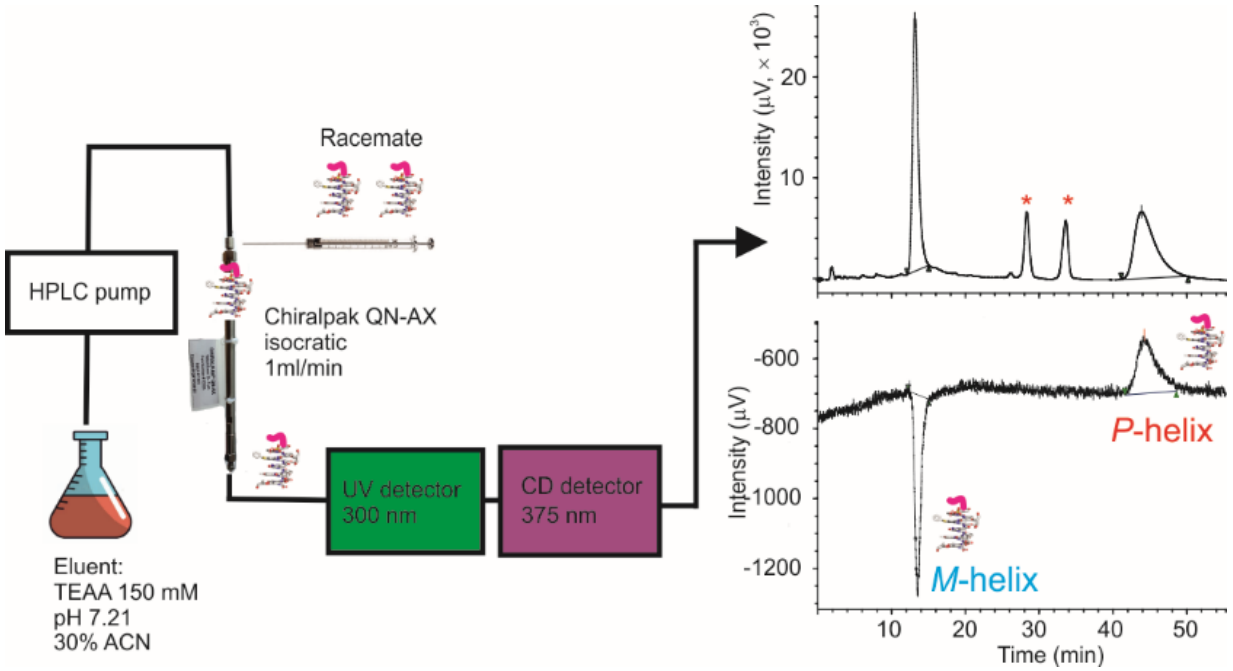

Figure S6. Scheme of the chiral RP-HPLC separation of the *P*- and *M*- conformers of biotinylated helical foldamer **1** on a chiral pack QN-AX® column from chiral technologies (Daicel) using isocratic conditions composed of CH_3CN in a trimethylammonium acetate (TEAA) buffer (150 mM, pH 7.21) (30:70, v/v) at a flow rate of 1 $mL.min^{-1}$ with a UV detection at 300 nm and a CD detection at 375 nm. The peak marked with red stars correspond to column impurities with no CD detection.

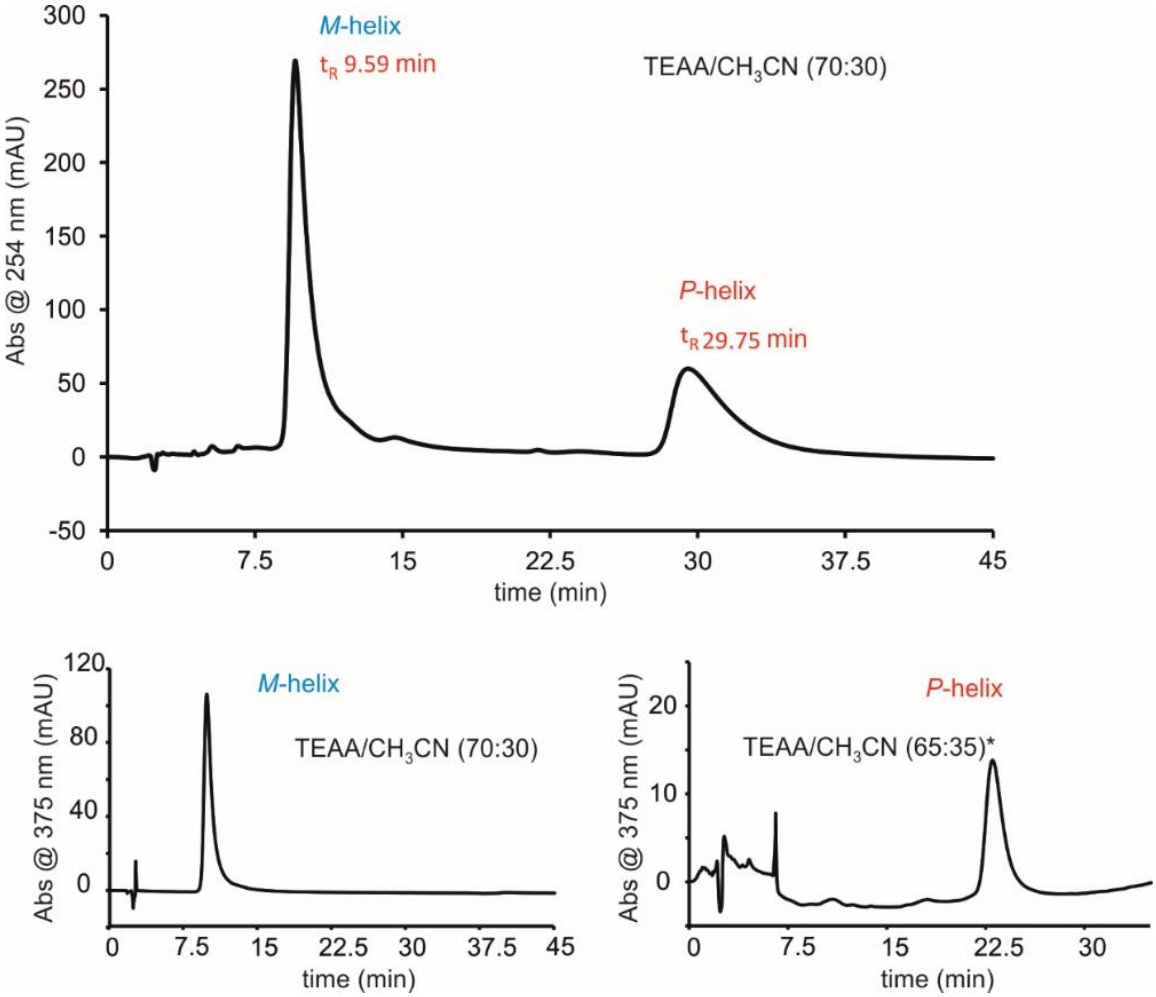

Figure S7. Example of chiral semi-preparative purification of the racemic mixture of compound **1** performed on an Ultimate 3000 Thermo HPLC line equipped with a fraction collector. Flow rate 1mL.min^{-1} detection and collect at 254 nm at 20 °C in the column oven. The HPLC profiles shown below correspond to the purified *M*- and *P*-helices. To sharpen the peak of the *P* conformer, we increased the ratio of CH_3CN (30%→35%) and consequently, the *P*-helix of **1** was eluted earlier.

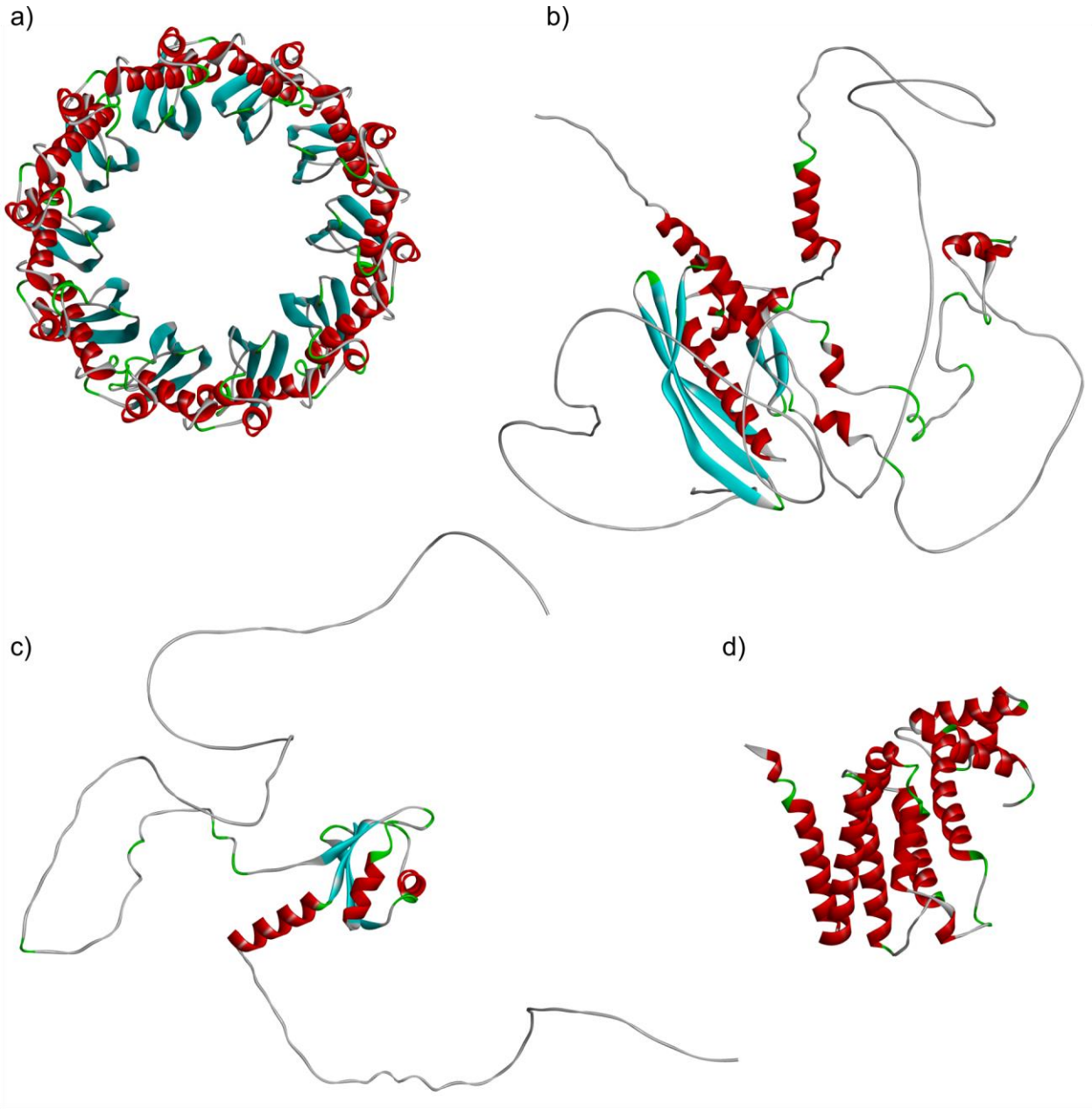

Figure S8. a) Cryo-EM structure of the decamer of yeast RAD52 (PDB #8G3G). b) AlphaFold model prediction of a full length monomer of yeast RAD52. b) AlphaFold model prediction of full length yeast SGN1. d) b) AlphaFold model prediction of full length yeast COQ9.

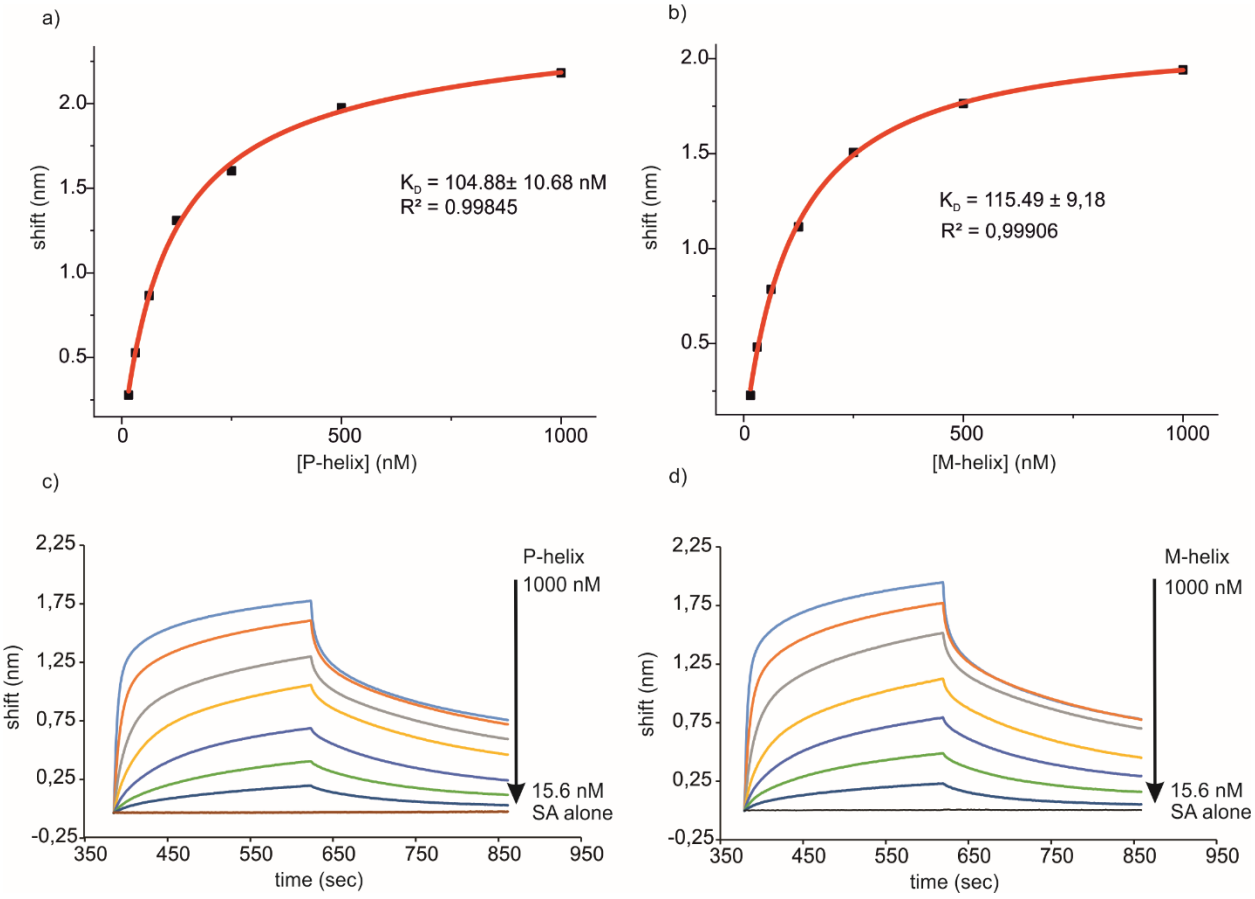

Figure S9. BLI assessment of the binding of SGN1 to *P*-**1** (a) and *M*-**1** (b) immobilized on streptavidin sensor tips. The graphs at the top show the curve fitting according to a 1:1 binding isotherm of the experimentally measured equilibrium response plotted against [SGN1]. A series of twofold dilutions of SGN1 was performed starting from 1000 nM. The real-time binding kinetics of both *M*-**1**/SGN1 and *P*-**1**/SGN1 interactions were characterized by rapid association (k_a) and dissociation (k_d) (graphs at the bottom). However, the fact that the curves keep climbing after the initial steep climb indicates some additional binding events. The dissociation constants (K_D) were estimated using the steady state model by fitting the signal response (y) as a function of protein concentration (x) to Langmuir's equation:

$$\boldsymbol{y = (Rmax * x)/(KD + X) + Ns * x}$$

where Ns represents the slope of the linear component corresponding to second phase binding event and Rmax, the maximum response.

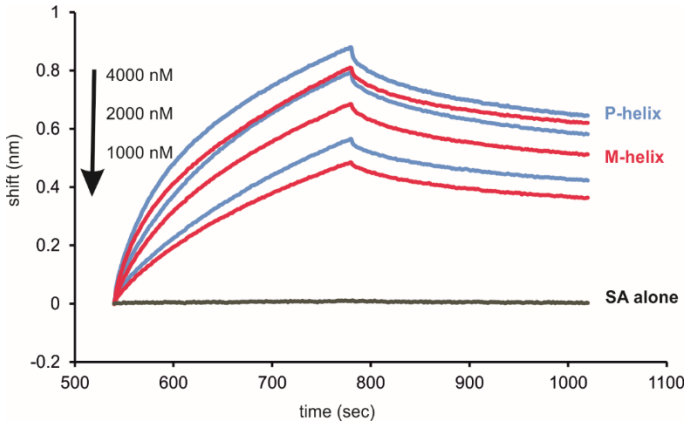

Figure S10. BLI assessment of the binding of COQ9 to *P*-**1** (blue) and *M*-**1** (red) immobilized on streptavidin sensor tips. Three different concentrations of COQ9 were assayed (4000 to 2000 nM) for each compound. A reference sensor tip was used to subtract the baseline and another to verify the absence of unspecific binding of COQ9 with the streptavidin (SA alone trace).

2. Experimental section

2.1. Materials and methods for chemical synthesis and characterizations

General: Chemical reagents were purchased from commercial suppliers (Sigma-Aldrich, Alfa-Aesar, and TCI) and used without further purification. Low loading Wang resin (100-200 mesh, manufacturer's loading: 0.41 mmol g^{-1}) was purchased from Sigma-Aldrich. 15-[D-(+)-Biotinylamino]-4,7,10,13-tetraoxapentadecanoic acid was purchased from Iris Biotech. Tetrahydrofuran (THF) and dichloromethane (DCM) were dried over alumina columns. *N*,*N*-diisopropylethylamine (DIPEA) was distilled over CaH_2 prior to use. Solid phase syntheses of foldamers were performed manually in open vessel mode using a CEM Discover microwave oven. HPLC grade acetonitrile and Milli-Q water were used for RP-HPLC analyses and purification. RP-HPLC analyses and purification were performed with JASCO HPLC systems (PU-2089 Plus, UV-2077 Plus, HV-2080-01, and AS-2055 Plus for analytical HPLC; DG-2080-53, PU-2086 Plus, and UV-2075 Plus for semi-preparative HPLC). 12.5 mM aqueous NH_4OAc-NH_4OH adjusted to pH 8.5 (solvent A) and pure acetonitrile (solvent B) were used as the mobile phase. RP-HPLC analyses were carried out on a Macherey-Nagel Nucleodur C18 HTec column (4×100 mm, 5 μm) at a flow rate of 1 mL min^{-1}. Semi-preparative RP-HPLC purifications were carried out on a Macherey-Nagel Nucleodur C18 HTec column (10×250 mm, 5 μm) at a flow rate of 3 mL.min^{-1}. Eluate from column was monitored by UV detection at 254 nm and 300 nm using a diode array detector. High-resolution electrospray mass spectra were recorded on a Thermo Exactive orbitrap instrument.
Chiral HPLC analyses were performed in reverse mode with JASCO HPLC systems (PU-2080-53 Plus, UV-2075 Plus, HV-2080-01, and AS-2055 Plus. A chiral QN-AX from Daicel was used for chiral separation of foldamer **1** at a flow rate of 1ml/min using a solvent mixture of 70 % of 120 mM TEAA buffer at pH 7.22 (solvent A) and 30% of pure acetonitrile. UV detection was recorded at 300 nm. A CD 1595 detector was mounted after the UV/Vis detector and CD detection was recorded at 400 nm.

Preparation of quinoline amino acid monomers for solid phase synthesis: Fmoc-protected 8-amino-quinoline-2-carboxylic acid monomers were prepared by using the methods previously reported.[1-2]

Solid phase foldamers synthesis: Conversion of low-loading Wang resin to bromomethyl Wang resin, loading of the first Fmoc-QAsp monomer, acid chloride activation of the monomers using Appel's reaction, automation of the SPFS and TFA cleavage were performed by using recently reported methodology.[3] Of note, the use of 2% DBU in NMP for Fmoc deprotection was recently optimized to two times 3 min (previously 2 × 10 min) and these conditions allowed us to skip the resin washing with 20% DIPEA in NMP after the Fmoc deprotection of the Q^{Sul} monomer that was prescribed in reference 1).

2.2. Methods for pull-down assay

Cell culture: Yeast cells BY4742 were grown aerobically at 28 °C in minimal medium (0.175% yeast nitrogen base without amino acids and ammonium sulfate, 0.5% ammonium sulfate, 0.1% potassium phosphate, 0.2% Drop-Mix, 0.01% of auxotrophic amino acids and nucleotide, pH 5.5), supplemented with 2% glucose as a carbon source. Cell growth was followed by optical density at 600 nm. For preparation of cell lysates, 5×10^7 cells were broken with glass beads in a buffer containing 0.6 M mannitol, 10 mM Tris

maleate, 2 mM EGTA, pH 6.8 plus protease inhibitor cocktail (Roche); lysates were centrifuged 10 min at 800 g. Lysates (supernatant) were kept frozen at −80 °C as aliquots until further uses.

Immobilization of biotinylated foldamers: 20 µL of resuspended Dynabeads™ MyOne™ Streptavidin T1(invitrogen) was transferred to a microcentrifuge tube and washed with 200 µL of PBS buffer (pH 7.4) four times. The beads were then incubated with 40 µL of 20 µM biotinylated foldamer for 60 min while shaking. The supernatant was subsequently discarded, and the beads were washed with 40 µL of PBS.

Enrichment of protein binders for foldamers: 15.39 µL of the yeast cell lysate (7.8 g/L) was diluted with 34.61 µL of PBS and then added to the washed beads. The resulting mixture was incubated for 20 min while shaking. The beads were then washed with 200 µL of PBS five times. To maximize enrichment, incubation of cell lysate and washing were repeated five more times.

Protein elution and digestion for mass spectrometry: Captured proteins were eluted off from the beads by incubation in 20 µL of 1× Laemmli sample buffer for 3 min at 100 °C. The eluate was then loaded onto a 10% SDS- PAGE gel, and SDS-PAGE was run for 5 min at 150 V. The resulting gel was stained with Coomassie blue for 1 h and subsequently destained with water. For reduction and alkylation, lanes for each replicate were first cut into small cubes (1×1×1 mm), and then incubated with destaining solution (25 mM ammonium bicarbonate in 50% CH_3CN) until bands were no longer visible. Destained gel pieces were collected and were subsequently incubated with 30 µL of 10 mM DTT solution for 30 min at 56 °C. The DTT solution was discarded, and the gels were then incubated with 30 µL of 100 mM iodoacetamide in 100 mM ammonium bicarbonate for 30 min in the dark. The iodoacetamide solution was removed, and the gels were subsequently dehydrated with CH_3CN. For in-gel digestion, the dehydrated gel pieces were submerged in a trypsin solution (5 µg of Trypsin (Promega) in 50 µL of 1 mM HCl and 450 µL of 50 mM ammonium bicarbonate) and incubated overnight at 37 °C. After the overnight digestion, 500 µL of 50 mM ammonium bicarbonate was added to the digestion mixture. The resulting supernatant was collected after 10 min incubation. 500 µL of an extraction solution (formic acid/CH_3CN/water, 5.0/47.5/47.5, v/v/v) was then added to gels, and the resulting supernatant was collected after 10 min incubation and combined with previously obtained supernatant. This process was repeated once again with 250 µL of the extraction solution. Extracted peptides were dried under reduced pressure and redissolved in 30 µL of 6% formic acid. Solution of extracted peptides was divided into three portions and analyzed separately.

nLC-MS/MS analysis and Label-Free Quantitative Data Analysis: Peptide mixture was analyzed on an Ultimate 3000 nanoLC system (Dionex, Amsterdam, The Netherlands) coupled to am Electrospray Orbitrap Fusion™ Lumos™ Tribrid™ Mass Spectrometer (Thermo Fisher Scientific, San Jose, CA). 10 µL of peptide digests were loaded onto the system. Peptides were separated on an analytical 75-mm id x 50-cm C18 Pep-Map column (LC Packings) with a 5–27.5% linear gradient of solvent B in 105 min (solvent A was 0.1% formic acid in water and solvent B was 0.1% formic acid in CH_3CN:water (8:2, v/v)) followed by a 10 min gradient from 27.5% to 40% solvent B. The mass spectrometer operated in positive ion mode and data were acquired using Xcalibur 4.1 software in a data-dependent mode. MS scans (m/z 375-1500) were recorded at a resolution of R = 120 000 (at m/z 200) with a dynamic exclusion set to 60 s. Fragmentation was limited to +2 to +7 charged ions and performed in HCD mode.

Database search and results processing: Data were searched by SEQUEST through Proteome Discoverer 1.4 (Thermo Fisher Scientific Inc.) against the saccharomyces cerevisiae Reference Proteome Set (from Uniprot 2017-10; 5991 entries). Spectra from peptides higher than 5000 Da or lower than 350 Da were rejected. The search parameters were as follows: mass accuracy of the monoisotopic peptide precursor and peptide fragments was set to 10 ppm and 0.6 Da respectively. Only b- and y-ions were considered for mass calculation. Oxidation of methionines (+16 Da) was considered as variable modification and carbamidomethylation of cysteines (+57 Da) as fixed modification. Two missed trypsin cleavages were allowed. Peptide validation was performed using Percolator algorithm[4] and only "high confidence" peptides were retained corresponding to a 1% False Positive Rate at peptide level.

Label-Free Quantitative Data Analysis: Label-free quantitation was performed thanks to Progenesis QI for Proteomics 2.0 (Nonlinear Dynamics Ltd, Newcastle, U.K). Calculation of protein abundance was the sum of the volume of corresponding peptides. A statistical test (ANOVA) was calculated for each group comparison and proteins were filtered based on p-value<0.05. Noticeably, only non-conflicting features and unique peptides were considered for calculation at protein level. Quantitative data were considered for proteins quantified by a minimum of 2 peptides. Relative quantitation was achieved by calculating the ratio of captured proteins (capture performed with foldamer bait) over control samples (same capture system but without foldamer bait).

Da Dalton
MS Mass Spectrometry
ppm Part per million
HCD Higher-energy Collisional Dissociation
SDS-PAGE Sodium Dodecyl Sulfate PolyAcrylamide Gel Electrophoresis

2.3. Recombinant protein expression and purification

Yeast DNA repair protein RAD52 homolog: The pET21a-yRad52 plasmid for yRad52 (UniProt accession number: P06778, aa 1 - 471) with a C-terminal hexa-histidine tag overexpression was obtained from Tomohiko Sugiyama (Ohio University). The full-length protein was expressed in E. coli BL21 Rosetta2 cells. Overnight pre-culture in Luria broth (LB) supplemented with 100 µg/ml ampicillin was diluted 1000-fold with fresh 4L LB media and grown at 37 °C until OD600 reached 1. The expression was induced by addition of isopropyl 1-thio-β-D-galactopyranoside to make the final concentration 0.75 mM, and the culture was incubated for 4 hours at 27 °C. Next, the cells were harvested at 6000 rpm (J-LITE® JLA-9.1000 Rotor, Beckman Coulter) and stored at −80 °C. The following purification steps were carried out at 4 °C. Briefly, the cells were resuspended in 60 mL of 50 mM PBS buffer pH 7.8 containing 2 mM 2-mercaptoethanol, 10% glycerol, 10 mM imidazole, and 1 mM PMSF. The cells were lysed by sonication and the lysate was clarified by centrifugation at 19000 rpm (JA-25.5 Rotor, Beckman Coulter) for 40 min. The supernatant was equilibrated with nickel-nitrilotriacetic acid (Ni-NTA) agarose beads by gentle mixing for 1 hour. The mixture was then applied to a gravity flow column, drained out, and washed with 50 mM Tris-HCl, pH 7.8 containing 100 mM imidazole. The protein was eluted with 50 mM Tris-HCl, pH 7.8, 250 mM imidazole, and immediately diluted with 50 mM Tris-HCl buffer to reduce the imidazole concentration to 100 mM. Finally, the protein was concentrated using a Vivaspin Turbo 4 column (100K MWCO), filtered

through a 0.2-µm filter, and loaded onto the gel filtration HiLoad 16/600 Superdex 200 column. Peak fractions were pooled together, concentrated, and frozen in liquid nitrogen prior to BLI measurements.

Yeast ubiquinone biosynthesis protein COQ9: The recombinant yeast COQ9 protein (UniProt accession number: Q05779, aa 36-256) with a C-terminal His6 tag was molecularly cloned into the expression vector pET24a and subsequently expressed in E. coli BL21 RIP Codon Plus cells. Briefly, cells previously cultured overnight in LB medium were diluted 1000-fold with fresh LB medium and cultured at 37 °C until an OD600 of 0.6-0.8 was reached. Induction of protein expression was initiated by the addition of 0.3 mM IPTG for 16 hours at 22 °C. After induction, cells were harvested by centrifugation at 8000g and stored at −20 °C until purification. Purification of the target protein was similar to that described for yRad52, except that TBS supplemented with 20mM imidazole was used for the washing step during IMAC purification.

Yeast RNA-binding protein SGN1: The gene encoding the SGN1 protein (UniProt accession number: P40561, amino acids 1 - 250) was cloned into the pMAL-c5e vector downstream of a maltose-binding protein (MBP), a His_{10} tag, and an HRV 3C cleavage site. Protein expression proceeded as follows: BL21 cells were transformed with the expression vector. Overnight cultures of BL21 cells were then inoculated into fresh LB media (4 L) supplemented with 100 µg/ml ampicillin. Expression induction occurred upon reaching an optical density at OD600 of 0.6, with the addition of 0.3 mM IPTG. The protein was expressed at 22 °C for 16 hours. Following expression, cells were harvested by centrifugation at 8000g and resuspended in a buffer containing 50 mM TRIS pH 7.4, 500 mM NaCl, 20 mM imidazole, 1 mM PMSF, and 1x Halt™ protease inhibitor cocktail. Cell were lysed by sonication, and subsequent centrifugation was conducted to eliminate cellular debris. Protein was purified by IMAC column. The target SGN1 protein was cleaved from the MBP-His10 tag-SGN1 fusion protein by digestion with HRV 3C protease at 4 °C overnight. Subsequently, a reverse IMAC column was employed to separate the cleaved MBP-His tag from the SGN1 protein. Finally, fractions containing the SGN1 protein from the reverse IMAC step were pooled and subjected to gel filtration chromatography using a HiLoad 16/600 Superdex 200 column.

2.4. Binding characterization by biolayer interferometry (BLI)

BLI experiments were performed on an Octet R8 instrument from Sartorius, following Sartorius recommendations. Prior to an assay, streptadvidin (SA) sensors were soaked for at least 10 min in phosphate buffer saline (1 × PBS). The kinetic experiment always starts with a baseline step over 60 s in 20 mM HEPES (pH 7.4, 150 mM NaCl, 0.02% Tween-20) buffer, followed by the loading of *P*- or *M*-foldamer isolated by chiral RP-HPLC isolated at 2 ug/mL over 120 s in HEPES. After foldamer ligand immobilization, the sensors were washed for 60 s in the same buffer, before to record a second baseline for 120 s, again in HEPES. Serial column dilutions (× 2) of the different proteins in HEPES were analysed, keeping the last well of the association column free of protein for referencing. Association lasted 240 s, followed by dissociation for another 240 s. The curves were fitted to binding models using the Octet analysis studio 13.0 software and replotted in Excel. Of note, the absence of unspecific binding of the proteins to streptavidin was confirmed by running a kinetic assay in a single well on a SA sensor with no immobilized foldamer at the highest screened protein concentration. For SGN1, the K_D value was calculated with the Langmuir's equation assuming a 1:1 binding model (see caption of Figure S8).

3. X-ray crystallographic analysis of compound 2

Lyophilized powder of **2** was dissolved using water and ammonium bicarbonate to a final concentration of 2mM. Crystallization trials were made using standard sitting drop vapor diffusion method at 293 K. X-ray quality crystals were obtained after three weeks by the addition of 0.75 µl of **2** and 1.25 µl of crystallization reagent composed of 50% w/v (+/-)-2-methyl-2,4-pentanediol, 50 mM HEPES buffer at pH 7.0, 80 mM potassium chloride, 10 mM magnesium sulphate in the reservoir. For low temperature diffraction measurement, a crystal was fished using a micro loop and plunged into liquid nitrogen. The mother liquor served as cryo-protectant for the crystal.

The X-ray diffraction data was collected at the micro-focus, fixed energy beamline ID30b[5] in European Synchrotron Radiation Facility (ESRF), Grenoble with a Dectris PILATUS3 X 2M detector. Diffraction data was measured at T = 100 K, λ = 0.8000 Å. The crystals were exposed for 0.02 s and 0.1° oscillation per frame. Diffraction data was processed using the program *XDS*[6]. The crystal belonged to the space group $P2_1/n$ with unit cell parameters: a = 35.903 (7) Å, b = 65.428 (13) Å, c = 36.158 (7) Å, α = 90°, β = 93.93 (3)°, γ = 90°; V = 84738 (30) Å^3 and 4 molecules per asymmetric unit (Z = 16, Z' = 4). The structure was solved with the program *SHELXT*[7] and refined by full-matrix least-squares method on F^2 with *SHELXL*-2014[8] within *Olex2*[9]. After each refinement step, visual inspection of the model and the electron-density maps were carried out using *Olex2*[9] and *Coot*[10] using $2F_o - F_c$ and difference Fourier ($F_o - F_c$) maps. The initial structure revealed all main-chain atoms of **2**. Few of the side chain atoms were refined with full or partial occupancy. AFIX, DFIX, SADI and FLAT instructions were used to improve the geometry of molecules. Restraints on anisotropic displacement parameters were implemented with RIGU and EADP instructions. All non-H atoms of the backbones were refined with anisotropic displacement parameters. From the difference Fourier map a molecule of (+/-)-2-methyl-2,4-pentanediol (MPD) was identified (from crystallization reagent). After several attempts to model the disordered side chains, the SQUEEZE[11] procedure was used to flatten the electron density map. Very disordered side chains and solvent molecules were removed. Calculated total potential solvent accessible void volume and electron count per cell are 34,860.6 Å^3 and 11,283 respectively. Hydrogen atoms were placed at idealized positions.

Statistics of data collection and refinement of **2** are described in Table S1. The final cif file of **2** was examined in IUCr's *checkCIF* algorithm. Due to the large volume fractions of disordered solvent molecules, weak diffraction intensity and poor resolution, a number of A- and B- level alerts remain in the *checkCIF* file. These alerts are inherent to the data set and refinement procedures. They are listed below and were divided into two groups. The first group demonstrates weak quality of the data and refinement statistics when compared to those expected for small molecule structures from highly diffracting crystals. The second group is concerned to decisions made during refinement and explained below. Atomic coordinates and structure factors of **2** was deposited in the Cambridge Crystallographic Data Centre (CCDC) with accession code 2280177. The data is available free of charge upon request (www.ccdc.cam.ac.uk/). Of note, Because of the large file size, the cif file could not be uploaded directly using the CDDC interface and was uploaded manually by CCDC staff. Consequently, the checkcif analysis could not be subjected to the direct insertion of comments and answers in the checkcif report, especially with respect to A-level alerts. These comments are therefore mentioned below.

CheckCIF validation of **2**:

Group 1 alerts (these illustrate weak quality of data and refinement statistics if compared to small molecule structures from highly diffracting crystals):

THETM01_ALERT_3_A The value of sine(theta_max)/wavelength is less than 0.550

Calculated sin(theta_max)/wavelength = 0.5208

PLAT082_ALERT_2_A High R1 Value ..... 0.22 Report

PLAT084_ALERT_3_A High wR2 Value (i.e. > 0.25) ..... 0.56 Report

PLAT097_ALERT_2_B Large Reported Max. (Positive) Residual Density 1.63 eA-3

PLAT201_ALERT_2_A Isotropic non-H Atoms in Main Residue(s) .....16 Report

PLAT241_ALERT_2_B High 'MainMol' Ueq as Compared to Neighbors of

PLAT242_ALERT_2_B Low 'MainMol' Ueq as Compared to Neighbors of

PLAT315_ALERT_2_B Singly Bonded Carbon Detected (H-atoms Missing)

PLAT316_ALERT_2_A Too many H on C in C=N Moiety in Main Residue .. Check

PLAT410_ALERT_2_A Short Intra H...H Contact

PLAT412_ALERT_2_B Short Intra XH3 .. XHn

PLAT430_ALERT_2_A Short Inter D...A Contact

PLAT733_ALERT_1_A Torsion Calc

Group 2 alert (is connected with decision made during refinement and explained below):

SHFSU01_ALERT_2_A The absolute value of parameter shift to su ratio > 0.20

Additional cycles of refinement did not remove this alert.

PLAT016_ALERT_5_A No _shelx_fab_file ..... Please Supply

Due to large file size, the file was separately supplied.

PLAT080_ALERT_2_A Maximum Shift/Error ..... 5.09 Why?

Additional cycles of refinement did not remove this alert.

PLAT202_ALERT_3_A Isotropic non-H Atoms in Anion/Solvent ..... 84 Check

Dummy O atom was introduced into refinement.

Table S1. Crystallographic data and refinement details for **2**.

Compound	**2**
Empirical formula	$C_{150.5}H_{111.1}N_{26.4}O_{33.8}S_3$
Formula weight	2925.2
Temperature	100 K
Wavelength	0.8000 Å
Crystal system	Monoclinic
Space group	$P2_1/n$
Unit cell dimensions	a = 35.903 (7) Å b = 65.428 (13) Å c = 36.158 (7) Å α = 90° β = 93.93 (3)° γ = 90°
Volume	84738 (30) Å^3
Z, Z'	16, 4
Density (calculated)	0.917 g/cm^3
Absorption coefficient	0.128 μ/mm^{-1}
Colour and shape	Yellow, blocks
Crystal size	0.120 x 0.100 x 0.005 mm
Index ranges	$-36 \leq h \leq 37$ $-67 \leq k \leq 66$ $-37 \leq l \leq 37$
Reflections collected	311527
R_{int}	0.1195
Data/restraints/parameters	97123/621/5266
Goodness-of-fit on F^2	2.426
Final R indexes [$I > 2\sigma(I)$]	R_1 = 0.2180 wR_2 = 0.5360
Final R indexes [all data]	R_1 = 0.2462 wR_2 = 0.5628
Largest diff. peak and hole	1.64/-1.33 e Å^{-3}
Total potential solvent accessible void volume from SQUEEZE	34860.6 Å^3
Electron count/cell	11283
CCDC #	2280177

4. Supplementary Data

Foldamer 1. Biotin-3-Amb-Q^{Sul}-Q^{Sul}-Q^{Dol}-Q^{Phe}-Q^{Leu}-Q^{Dap}-Q^{Dap}-Q^{Asp}-Q^{Orn}-Q^{Hyd}-Q^{Dol}-Q^{Asp}-OH

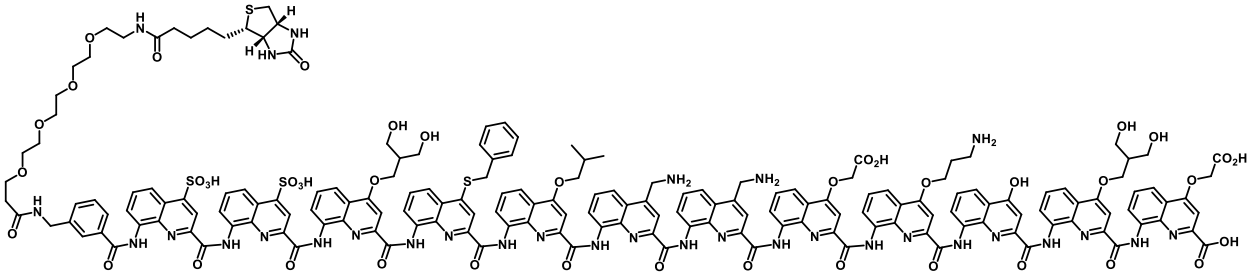

Foldamer **1** was synthesized on a low loading Wang resin (7.19 μmol). The crude product obtained from cleavage was purified by RP-HPLC (22-28% solvent B, over 19 min) to afford the title compound as a yellow solid (6.5 mg, 25.7%, purity by RP-HPLC: >99%). HRMS (ESI^-): *m/z* calcd for $C_{177}H_{161}N_{31}O_{42}S_4$ $[M-2H]^{2-}$ 1760.5171 found 1760.5206; *m/z* calcd for $C_{177}H_{160}N_{31}O_{42}S_4$ $[M-3H]^{3-}$ 1173.3423 found 1173.3473.

Foldamer 2. Ac-Q^{Sul}-Q^{Sul}-Q^{Dol}-Q^{Phe}-Q^{Leu}-Q^{Dap}-Q^{Dap}-Q^{Asp}-Q^{Orn}-Q^{Hyd}-Q^{Dol}-Q^{Asp}-OH

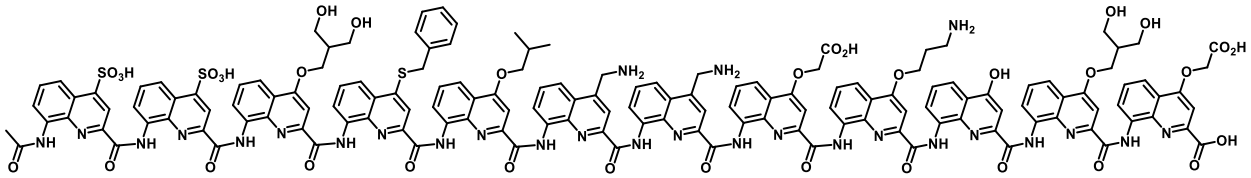

Foldamer **2** was synthesized on a low loading Wang resin (0.78 μmol). The crude product obtained from cleavage was purified by RP-HPLC (20-27% solvent B, over 19 min) to afford the title compound as a yellow solid (0.7 mg, 30.3%, purity by RP-HPLC: 98.34%). HRMS (ESI^-): *m/z* calcd for $C_{150}H_{121}N_{27}O_{35}S_3$ $[M-2H]^{2-}$ 1478.3863 found 1478.3890; *m/z* calcd for $C_{150}H_{120}N_{27}O_{35}S_3$ $[M-3H]^{3-}$ 985.2551 found 985.2584.

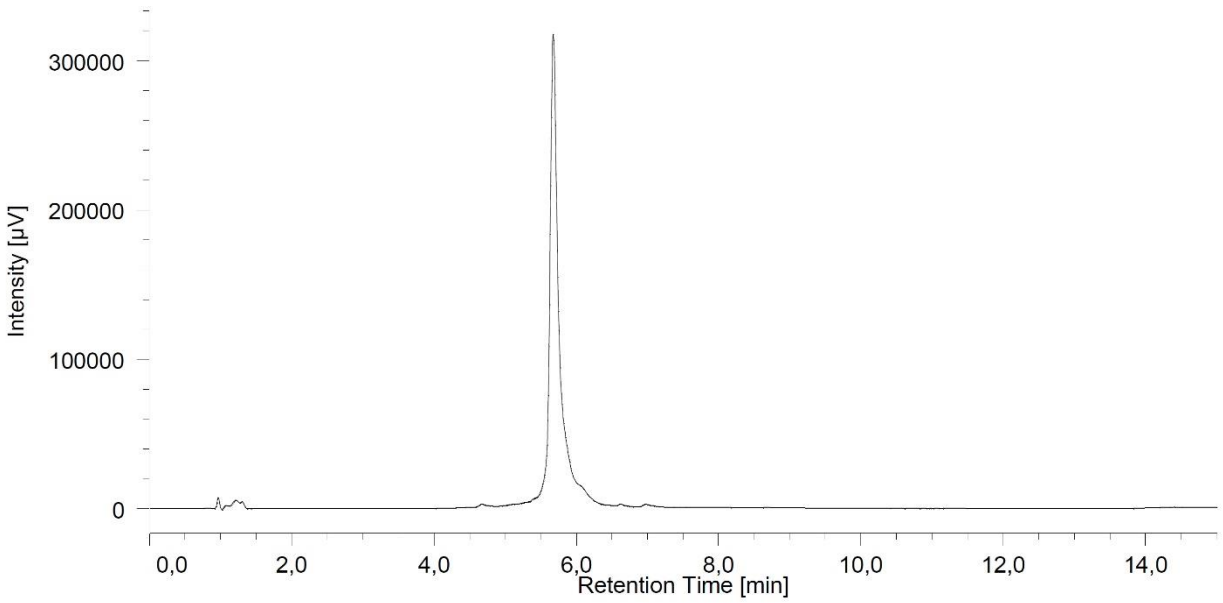

Figure S11. Analytical RP-HPLC (10-60% solvent B, over 12 min) trace of foldamer **1**.

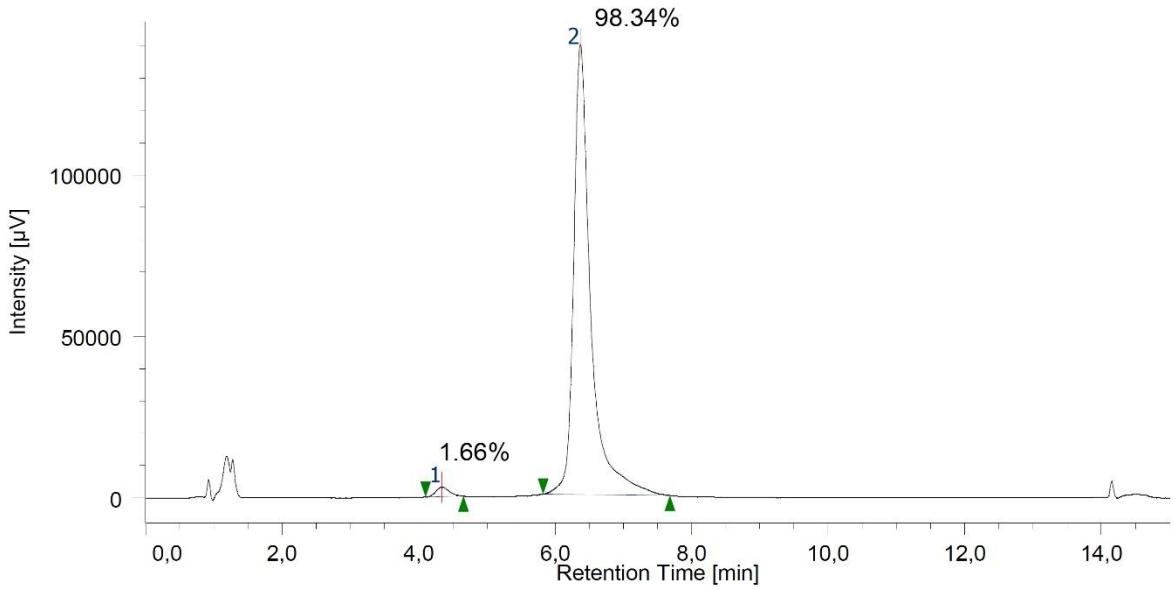

Figure S12. Analytical RP-HPLC (20-30% solvent B, over 12 min) trace of foldamer **2**.

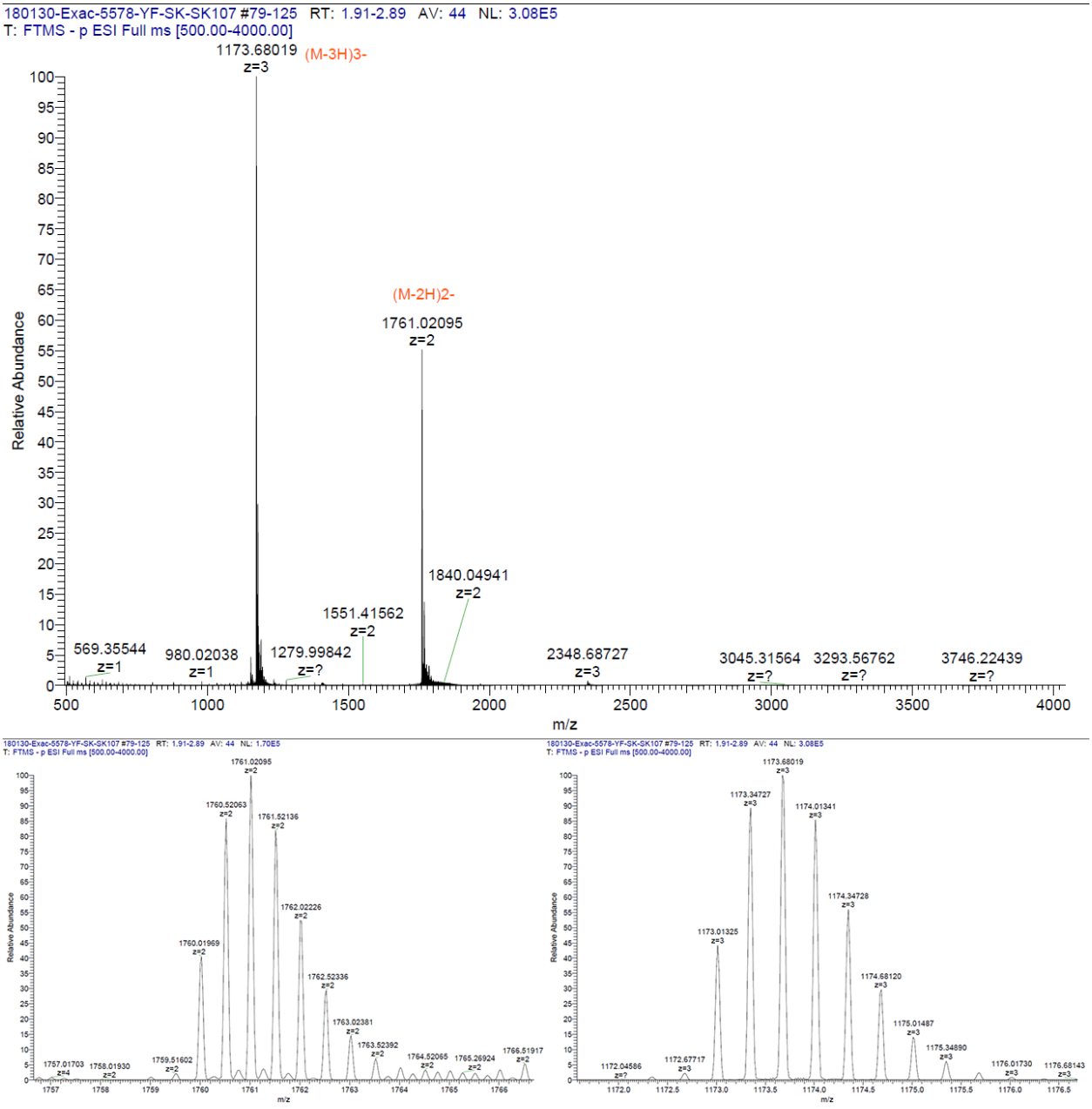

Figure S13. HR-MS spectrum of foldamer **1**.

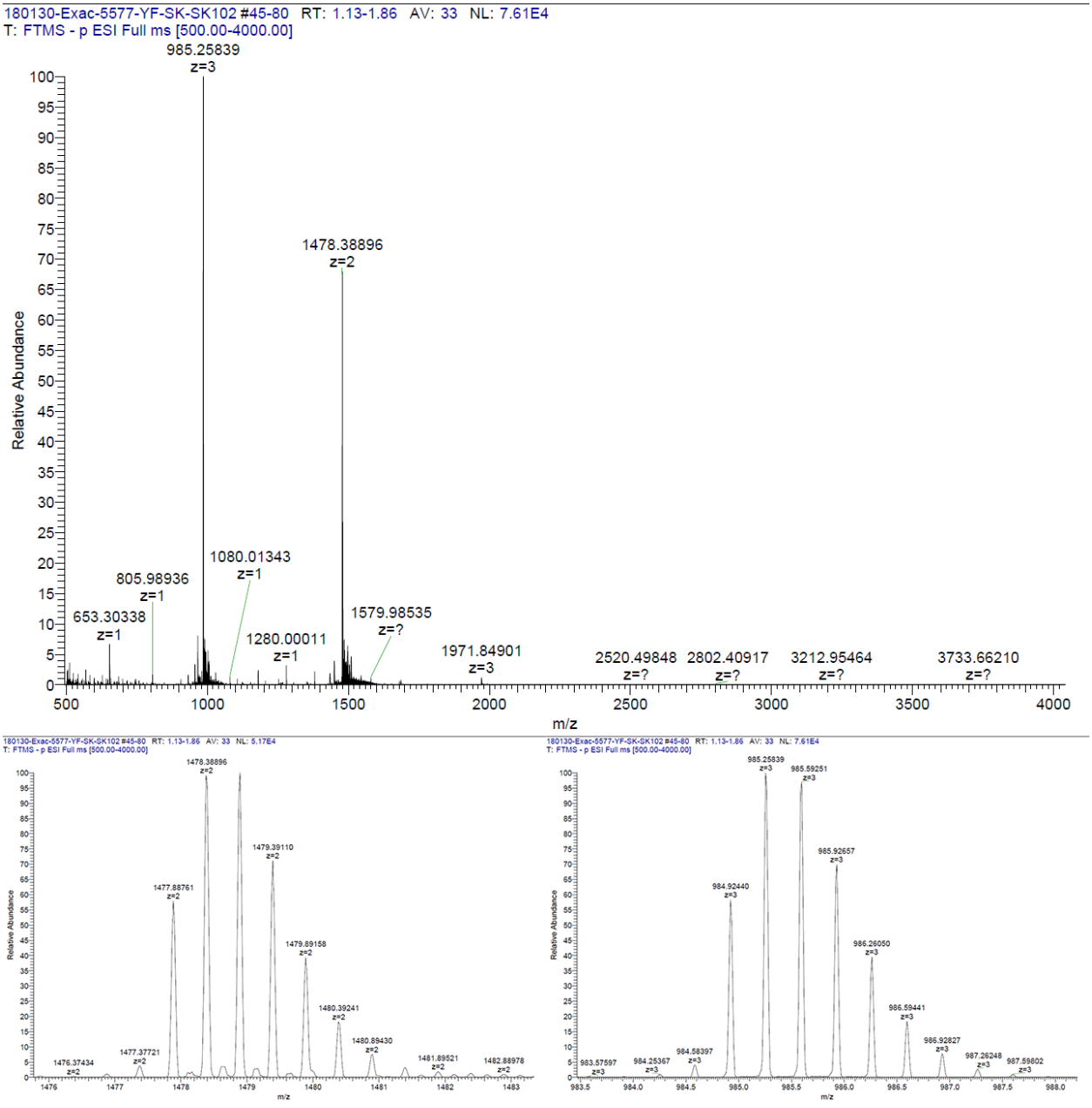

Figure S14. HR-MS spectrum of foldamer **2**.

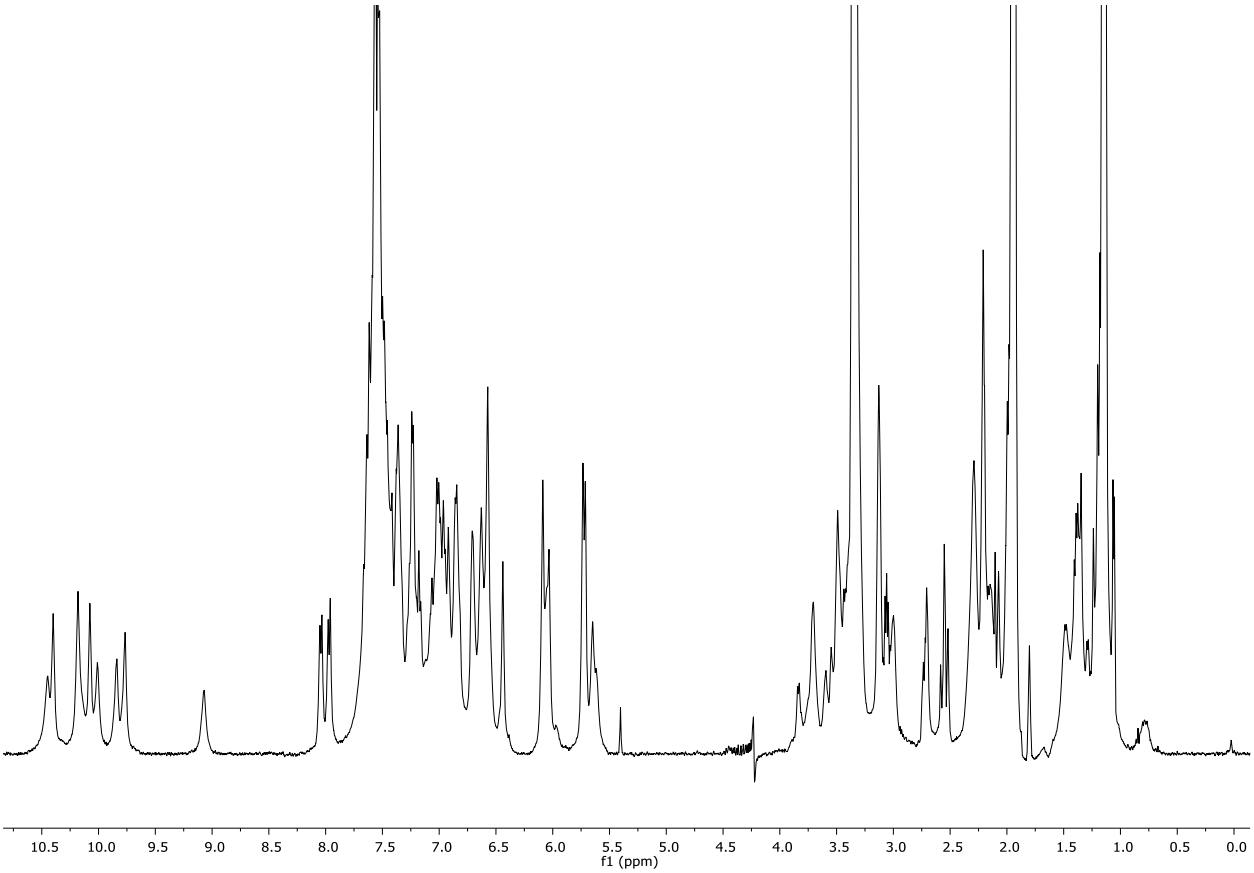

Figure S15 ^{1}H NMR spectrum of foldamer **1** (500 MHz, CD_3CN + 50% H_2O, water suppression), 25 °C.

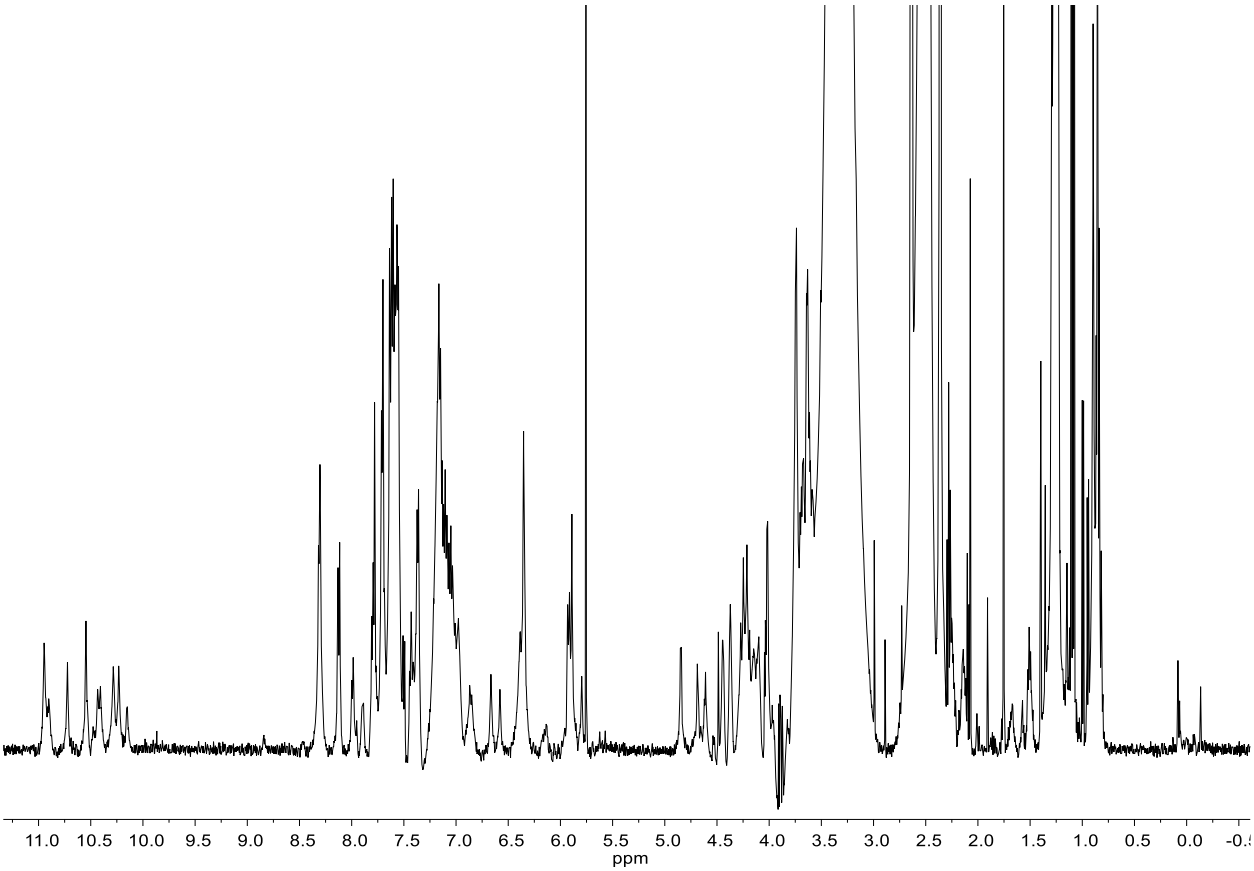

Figure S16 ^{1}H NMR spectrum of foldamer **2** (500 MHz, DMSO-d_6), 25 °C.

5. References

1. Hu, S. J. Dawson, P. K. Mandal, X. de Hatten, B. Baptiste and I. Huc, *Chem. Sci.*, 2017, **8**, 3741−3749.
2. S. De, B. Chi, T. Granier, T. Qi, V. Maurizot and I. Huc, *Nat. Chem.*, 2018, **10**, 51−57.
3. a) V. Corvaglia, F. Sanchez, F. S. Menke, C. Douat and I. Huc, *Chem. Eur. J.*, 2023, e202300898 ; b) B. Baptiste, C. Douat-Casassus, K. Laxmi-Reddy, F. Godde and I. Huc, *J. Org. Chem.*, 2010, **75**, 7175−7185.
4. L. Käll, J. D. Canterbury, J. Weston, W. S. Noble and M. J. MacCoss, *Nat. Methods*, 2007, **4**, 923−925.
5. A.A. McCarthy, R. Barrett, A. Beteva, H. Caserotto, F. Dobias, F. Felisaz, T. Giraud, M. Guijarro, R. Janocha, A. Khadrouche, M. Lentini, G.A. Leonard, M. Lopez Marrero, S. Malbet-Monaco, S. McSweeney, D. Nurizzo, G. Papp, C. Rossi, J. Sinoir, C. Sorez, J. Surr, O. Svensson, U. Zander, F. Cipriani, P. Theveneau and C. Mueller-Dieckmann, *J. Synchrotron Radiat.*, 2018, **25**, 1249−1260.
6. W. Kabsch, *Acta Crystallogr. Sect. D-Biol. Crystallogr.*, 2010, **66**, 125−132.
7. G.M. Sheldrick, *Acta Crystallogr. Sect. A*, 2015, **71**, 3−8.
8. G.M. Sheldrick, *Acta Crystallogr. Sect. C-Struct. Chem.*, 2015, **71**, 3−8.
9. O.V. Dolomanov, L.J. Bourhis, R.J. Gildea, J.A.K. Howard and H. Puschmann, *J. Appl. Crystallogr.*, 2009, **42**, 339−341.
10. P. Emsley, B. Lohkamp, W.G. Scott and K. Cowtan, *Acta Crystallogr. Sect. D-Biol. Crystallogr.*, 2010, **66**, 486−501.
11. A.L. Spek, *Acta Crystallogr. Sect. D-Struct. Biol.*, 2009, **65**, 148−155.